The secondary electron yield of noble metal surfaces

L. A. Gonzalez, M. Angelucci, R. Larciprete, and R. Cimino

The secondary electron yield of noble metal surfaces

L. A. Gonzalez,[1,2] M. Angelucci,[1] R. Larciprete,[1,3] and R. Cimino[1,2,a]

[1]*LNF-INFN, P.O. box 13, 00044 Frascati, Roma, Italy*
[2]*CERN, CH-1211 Geneva 23, Switzerland*
[3]*CNR-ISC Istituto dei Sistemi Complessi, via dei Taurini 19, 00185 Roma, Italy*

Secondary electron yield (SEY) curves in the 0-1000 eV range were measured on polycrystalline Ag, Au and Cu samples. The metals were examined as introduced in the ultra-high vacuum chamber and after having been cleaned by Ar^+ ion sputtering. The comparison between the curves measured on the clean samples and in the presence of contaminants, due to the permanence in atmosphere, confirmed that the SEY behavior is strongly influenced by the chemical state of the metal surface. We show that when using very slow primary electrons the sample work function can be determined with high accuracy from the SEY curves. Moreover we prove that SEY is highly sensitive to the presence of adsorbates even at submonolayer coverage. Results showing the effect of small quantities of CO adsorbed on copper are presented. Our findings demonstrate that SEY, besides being an indispensable mean to qualify technical materials in many technological fields, can be also used as a flexible and advantageous diagnostics to probe surfaces and interfaces. *© 2017 Author(s). All article content, except where otherwise noted, is licensed under a Creative Commons Attribution (CC BY) license (http://creativecommons.org/licenses/by/4.0/).* https://doi.org/10.1063/1.5000118

I. INTRODUCTION

The accurate determination of the secondary electron yield (SEY) of the materials exposed to radiation is a key issue in the technical design of new particle accelerators.[1–6] The prevision and the minimization of SEY is a strict requirement to limit electron cloud phenomena and favor the stability of machine performances.[7–9] Analogous criticality concerns microwave and RF components for space applications that find one of their most important functional limitations in the multipactor and corona breakdown discharges.[10] The urgency of these questions has led to diffuse investigations and now the importance of the factors related to intrinsic material properties,[11,12] morphology (roughness, structural disorder),[13,14] chemical state (reactivity, passivation, contamination)[15] and temperature (gas adsorption)[16,17] in determining the actual SEY behavior of materials hit by electron fluxes has been well assessed.

Usually for a sample exposed to an electron beam the SEY curve is evaluated in terms of the standard parameters that describe the overall response of the material to external excitation, δ_{max}, E_{max} and $E_{0,1}$,[6] i. e. the maximum of the SEY curve, the corresponding primary electron energy and the first crossover energy at which the SEY crosses unit. In this approach the very low energy part of the SEY curve is currently neglected essentially because its contribution to the total SEY is not quantitatively relevant.

In this study we measured SEY and LE-SEY curves of metal samples introduced in UHV from the atmosphere that mimic the real surfaces of machine or device components and compare the results with the curves measured on the corresponding surface cleaned in UHV. Whereas the behavior observed at high primary electron energy confirm the trend already well documented in the literature, the additional information provided in the LE-SEY region qualifies this technique as a fast and effective tool to characterize the cleanliness of the sample. Moreover we investigated

---

[a]Corresponding author: roberto.cimino@lnf.infn.it.

the modification induced in the LE-SEY and SEY curves by controlled low temperature (~10 K) adsorption of the residual gases and of carbon monoxide (CO), highlighting the effects due to surface adsorbates even at submonolayer coverage.

II. EXPERIMENTAL

The experiment was performed at the Material Science INFN-LNF laboratory, in a μ-metal chamber with less than 5 mGauss residual magnetic field at the sample position, under ultra high vacuum (UHV) conditions, with a background pressure below 2×10^{-10} mbar.[13,18] Polycrystalline Cu, Au and Ag samples, were introduced in the UHV chamber from atmosphere and without any chemical cleaning. We characterized such "as received" technical surfaces by XPS and SEY measurements. Afterwards, sample cleaning was carried out by repeated Ar$^+$ sputtering cycles at 1.5 KeV in Ar pressure of 5×10^{-6} until no signal of C and O was observed in the XPS spectrum. In the following we name "clean" the metal surfaces that were Ar$^+$ ion sputtered in UHV and "as received" the surfaces of the samples just introduced from atmosphere that were examined without any *in situ* cleaning procedure. XPS measurements were performed by using an Omicron EA125 analyzer to reveal the photoelectrons excited by the non monochromatic radiation of an Mg Kα (hν=1253.6 eV) source). The SEY is defined as the ratio of the number of electrons leaving the sample surface I_{out} to the number of incident electrons I_p per unit area. Since $I_{out} = I_p - I_s$, where I_s is the sample current to ground, then:

$$SEY = \delta = \frac{I_{out}}{I_p} = \frac{I_p - I_s}{I_p} = 1 - \frac{I_s}{I_p} \qquad (1)$$

To obtain the SEY, I_p(some tens of nA) was measured by means of a Faraday cup positively biased in order to prevent backscattered reemission to vacuum, whereas negative a bias voltage of $V_s = -75V$ was applied to the sample to determine I_s. SEY was measured as a function of the primary electron energy. The energy scan was performed with a variable step size from 0.1 to 10 eV. For this study we used an ELG-2 Kimball Physics e-gun, which uses a standard Ta disc cathode. Electrons are emitted from the cathode by means of thermionic emission and irradiate the sample with a <1mm diameter spot. The energetic distribution of the beam electron beam can be assumed to have a Gaussian shape with an energy width FWHM$_g$ of about 0.85 eV, depending on the cathode temperature. During the measurement of an entire SEY curve, a total dose of 10^{-6} C/mm^2 is applied onto the surface, which is known to have a negligible effect in terms of electron conditioning.[8,15] The geometry of the experimental set-up as well as the electron gun working conditions (cathode temperature and V_{bias}) were kept constant during the whole experiment.

III. RESULTS AND DISCUSSION

The SEY curves measured on "as received" Au, Ag and Cu samples are shown by the red lines in Fig.1. The curves exhibit the typical line shape measured for metal surfaces examined before being cleaned in UHV. In fact, for all metals the SEY rapidly rises with increasing E$_p$ up to ~ 200 eV and decreases for higher primary energies. The δ_{max} values measured for Ag, Au and Cu are 2.7, 2.0 and 2.1, respectively. In all cases the XPS spectra exhibit very intense O1s and C 1s core level peaks (see below), which are determined by the presence of surface contamination due to the permanence of the samples in atmosphere.

After surface cleaning by Ar$^+$ sputtering the level of contamination is brought below the XPS detection limit and correspondingly the SEY decreases for all three metals. The resulting curves show values close to zero at very low E$_p$ and remain well below 1.7 in the whole primary energy range. In particular Cu shows the lowest δ_{max} (1.3), whereas moderately higher values are measured for Ag (δ_{max}=1.65) and Au (δ_{max}=1.70), in good agreement with previously published results.[19,20]

More interesting results are observed in the very low E$_p$ range. Fig.2 shows the SEY curves of the "as received" and clean Ag, Au and Cu surfaces. For E$_p \leq 18$ eV a 0.1 eV step size was used to measure all details within the experimental resolution, while at higher energies a bigger energy step
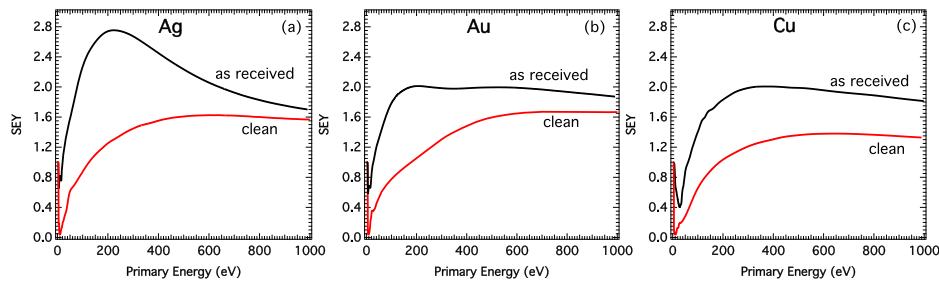
FIG. 1. Comparisons between the SEY curves measured for clean (black line) and as received (red line) surfaces of a) Ag b) Au c) Cu polycrystalline samples. In all cases the primary energy is referred to the Fermi level.
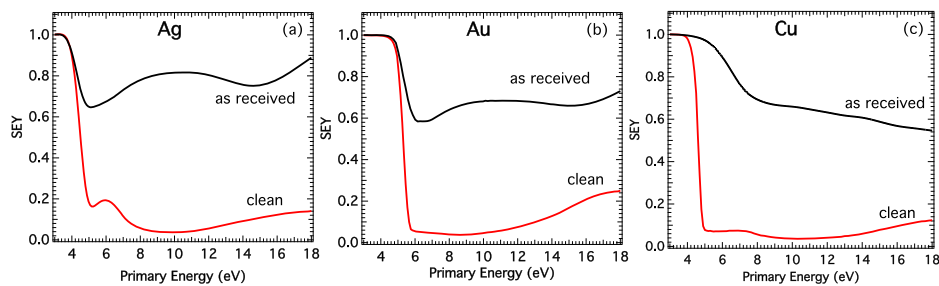

FIG. 2. Comparisons between the LE-SEY curves measured for clean (black line) and as received (red line) surfaces of a) Ag b) Au c) Cu polycrystalline samples. In all cases the primary energy is referred to the Fermi Level.

was used to minimize sample electron doses. All clean metals show a sharp drop from 1 to values close to zero within an energy region smaller than 1 eV. This behavior indicates the transition from the regime where the incident electron beam is totally backscattered ($I_s = 0$) to the regime where part of it is transmitted through the sample. ($I_s \geq 0$) The sharp transition then gives the vacuum level position for each sample. The experimental energy width of the transition is determined by the energy width of the primary electron beam. By analyzing the SEY curves we could estimate that the transition widths are ∼ 0.85 eV, in agreement with the thermally broadened beam emitted by the thermoionic cathode. During each SEY measurement particular care was dedicated to the calibration of the sample bias voltage. Then, the energy separations found between the Ag and Au and Cu vacuum levels provide the differences between the corresponding metal work functions, being the Fermi level a common reference for the system. Once set the Cu work function to 4.6 eV the values derived for Au and Ag result 5.3 and 4.4 eV, respectively, in good agreement with the literature.[21]

In the 6-8 eV wide regions above the transition energy, the SEY values remain quite low for all clean metals. These nearly flat curves are similar to the typical reflectivity curves measured for single crystal[22] and polycrystalline metals[23] in agreement with the fact that for E_p a few eV higher than the vacuum level, the efficiency of generating secondary electrons that escape from the solid is very low.[3,24]

When moving to the "as received" samples, Fig.2 shows that for E_p above the transition region, the SEY remains higher than 0.5 for all metals. Clearly, the presence of chemisorbed compounds, which modify the chemical bonds at the metal surface and, most importantly, interact directly with the impinging electrons, strongly affects the LE-SEY curves. In these cases, due to the complexity of the electron-surface interaction, it is not straightforward to disentangle the different processes and elucidate the origin of the observed modification. Even the features due to electron reflectivity which appear in the LE-SEY curves in general are barely assigned, since subtle differences in the support and/or adsorbate properties might significantly change the observed trend.[23,25–28] Nevertheless, a qualitative analysis of the results may lead to reasonable conclusions. The similar
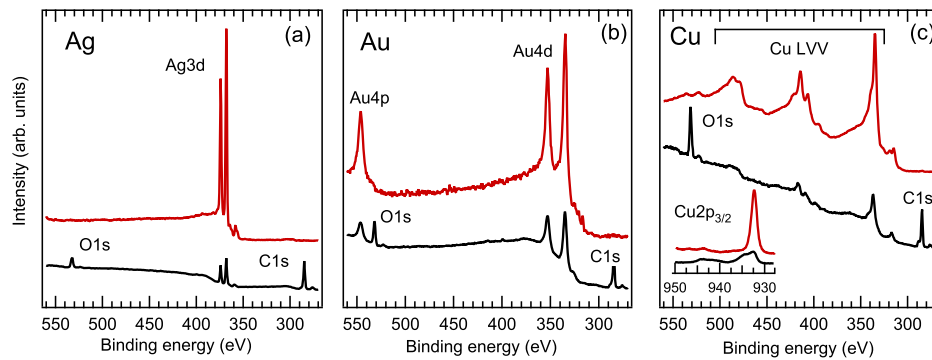
FIG. 3. XPS spectra measured on "as received" (red lines) and Ar$^+$ sputtered (black lines) a) Ag, b) Au and c) Cu polycrystalline samples. The inset in Fig.3c compares the high resolution spectra measured in the Cu2p$_{3/2}$ spectral region.

curves measured for Ag and Au, which show a minimum in proximity of the transition region followed by a ~ 6 eV wide maximum and by a second minimum, suggest the presence of a similar contaminating layer which dominates the overall sample behavior. Differently, in the case of Cu a continuous SEY decrease together with a net increase of the work function suggests a different chemical environment. The XPS spectra measured on the "as received" metals and compared in Fig.3 sustain this hypothesis. In fact, the O1s/C1s intensity ratio, that is of the order of 0.6-0-8 for Au and Ag, rises to 1.4 in the case of Cu, suggesting the occurrence of metal oxidation. This is confirmed by the Cu2p$_{3/2}$ line shape showing a dominating oxide phase (see inset in Fig.3c). Such a profound modification of the metal chemical state is not observed for the less reactive Au and Ag surfaces whose Au4d and Ag3d spectra measured on the "as received" surfaces show a lower intensity but a similar line shape with respect to the clean metals. The formation of a oxidized near surface layer in the Cu sample is likely responsible for the work function increase[29] observed in Fig.2c.

The important effect that surface contaminants have on the measured SEY, even in the absence of surface oxidation, is well exemplified in Figs.4a and 4b which shows the SEY curves measured at 10 K in the 0-35 eV and 0-900 eV ranges respectively, on the Cu sample clean and in the presence of controlled adsorbate layers. The corresponding curves measured at RT are also shown for
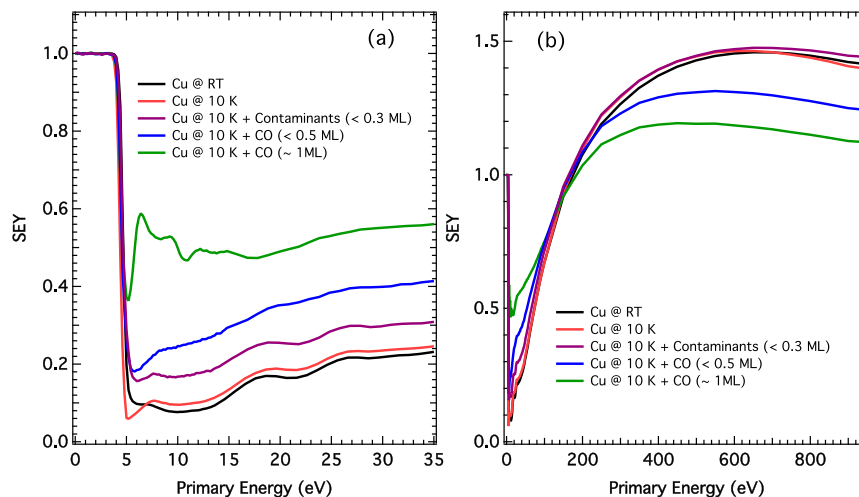

FIG. 4. a) LE-SEY and b) SEY curves measured at 10 K on a polycrystalline Cu sample clean (red) and in the presence of 0.3 ML of adsorbed residual gases (purple) and of of 0.5 ML (blue) and 1 ML (green) of adsorbed CO. The LE-SEY and SEY curves measured on the clean sample at RT are shown for comparison (black). In all cases the primary energy is referred to the Fermi level.

comparison. The similarity between the curves measured on the clean metal at RT and at 10 K proves that cooling down the sample does not determine any significant SEY variation. Keeping the sample at low temperature for some time determines the progressive adsorption of residual gas molecules (mainly H_2O, CO, CO_2 and CH_4). The presence of such contaminants at a coverage estimated of the order of 0.3 ML modifies only the LE-SEY region which slightly increases with respect to the clean surface. A stronger effect is observed when the clean metal is dosed with CO. In this case δ_{max} decreases with increasing coverage, becoming 1.3 and 1.2 after the adsorption of 0.5 and 1 ML of CO, respectively, whereas an inverse behavior is observed in the LE-SEY region. The opposite high- and low-energy trends can be reconciled by assuming that the presence of the adsorbed molecules reduces the number of low energy electron penetrating into the sample[30] due to enhanced surface scattering and decreases the yield of the emitted secondary electrons.

The fine structures which appear in the LE-SEY curve measured at CO coverage of 1 ML[31] will be the subject or a future investigation. The comparison between the curves taken with and without adsorbed CO indicates that a coverage of 1 ML is sufficient to deeply modify the LE-SEY curve proving the high surface sensitivity of this technique. Further studies in this direction could contribute to the understanding of the behavior of the inelastic mean free path for very slow electrons as discussed in recent experimental investigations.[32,33] Our data clearly show that, in addition to the possibility of investigating very low energies SEY, this type of measurements enables to determine the work function of materials[34] (once a reference work function has been measured) with an estimated resolution of about 100 meV. Such resolution essentially depends on the bias and on the primary electron voltage stability and reproducibility.

IV. CONCLUSIONS

In summary we have shown that the surface chemical state is a key factor in determining the metal SEY and LE-SEY curves. Whereas clean metals exhibit SEY values that do not exceed 1.6 and are even lower in the case of copper, the presence of a contaminating layer can rise δ_{max} well above 2 while shifting the maximum of the SEY curves below 400 eV. More interestingly, the LE-SEY curves show heavy changes in the presence of adsorbates even at submonolayer coverage. Our results demonstrate that for very slow electrons the LE-SEY curve allows an easy measurement of the sample work function. Then SEY and LE-SEY are valid spectroscopic tools, that, with a limited experimental requirement, can be used both to determine the response of materials to external excitation in terms of secondary electrons emission and also as flexible and sensitive diagnostics to state surface cleanliness and to follow surface reactions, desorption and ultrathin layer growth.

[1] A. W. Chao, K. H. Mess, M., and F. Zimmermann, eds., *The Oxford Handbook of Innovation* (World Scientific Publishing Co Pte Ltd, 2013).
[2] F. Zimmermann, "Review of single bunch instabilities driven by an electron cloud," Phys. Rev. ST Accel. Beams **7**, 124801 (2004).
[3] R. Cimino, I. Collins, M. A. Furman, M. Pivi, F. Ruggiero, G. Rumolo, and F. Zimmermann, "Can low-energy electrons affect high-energy physics accelerators?," Phys. Rev. Lett. **93**, 014801 (2004).
[4] O. Domínguez, K. Li, G. Arduini, E. Métral, G. Rumolo, F. Zimmermann, and H. M. Cuna, "First electron-cloud studies at the Large Hadron Collider," Phys. Rev. ST Accel. Beams **16**, 011003 (2013).
[5] Proc. ECLOUD12 (La Biodola, Isola d'Elba, Italy), http://ecloud12.web.cern.ch/ecloud12/ (2012).
[6] R. Cimino and T. Demma, "Electron cloud in accelerators," Int. J. Mod. Phys. A **29**, 1430023 (2014).
[7] M. Pivi, G. Collet, F. King, R. E. Kirby, T. Markiewicz, T. O. Raubenheimer, J. Seeman, and F. LePimpec, "Experimental observations of in situ secondary electron yield reduction in the PEP-II particle accelerator beamline," Nucl. Instr. and Meth. A **621**, 47–56 (1995).

[8] R. Cimino, D. Grosso, M. Commisso, R. Flammini, and R. Larciprete, "Nature of the decrease of the secondary-electron yield by electron bombardment and its energy dependence," Phys. Rev. Lett. **3**, 2098 (2012).

[9] R. Cimino, V. Baglin, and F. Schäfers, "Potential remedies for the high synchrotron-radiation-induced heat load for future highest-energy-proton circular colliders," Phys. Rev. Lett. **115**, 264804 (2015).

[10] S. T. Lai, *Fundamentals of Spacecraft Charging: Spacecraft Interactions with Space Plasmas* (Princeton, NJ, 2002).

[11] C. Y. Vallgren, G. Arduini, J. Bauche, S. Calatroni, P. Chiggiato, K. Cornelis, P. C. Pinto, B. Henrist, E. Mètral, H. Neupert, G. Rumolo, E. Shaposhnikova, and M. Taborelli, "Amorphous carbon coatings for the mitigation of electron cloud in the CERN Super Proton Synchrotron," Phys. Rev. ST Accel. Beams **14**, 071001 (2011).

[12] R. Larciprete, D. Grosso, A. D. Trolio, and R. Cimino, "Evolution of the secondary electron emission during the graphitization of thin C films," App. Surf. Sci. **328**, 356–360 (2015).

[13] L. Gonzalez, R. Larciprete, and R. Cimino, "The effect of structural disorder on the secondary electron emission of graphite," AIP Advances **6**, 095117 (2016).

[14] R. Valizadeh, Malyshev, S. Wang, B.-T. Sian, Cropper, and N. Sykes, "Reduction of secondary electron yield for e-cloud mitigation by laser ablation surface engineering," Appl. Surf. Sci. **404**, 370–379 (2017).

[15] R. Larciprete, D. Grosso, M. Commisso, R. Flammini, and R. Cimino, "Secondary electron yield of Cu technical surfaces: Dependence on electron irradiation," Phys. Rev. ST Accel. Beams **16**, 011002 (2013).

[16] J. Cazaux, Y. Bozhko, and N. Hilleret, "Electron-induced secondary electron emission yield from condensed rare gases: Ne, Ar, Kr and Xe," Phys. Rev. B **71**, 035419 (2005).

[17] A. Kuzucan, H. Neupert, M. Taborelli, and H. Störi, "Secondary electron yield on cryogenic surfaces as a function of physisorbed gases," J. Vac. Sci. Technol. A **30**, 051401 (2012).

[18] R. Cimino, L. Gonzalez, R. Larciprete, A. Di Gaspare, G. Iadarola, and G. Rumolo, "Detailed investigation of the low energy secondary electron yield of technical Cu and its relevance for the LHC," Phys. Rev. ST Accel. Beams **18**, 051002 (2015).

[19] I. Bronshtein and B. Graiman, *Secondary Electron Emission* (Nauka, Moscow, 1969).

[20] H. Bruining and J. H. De Boer, "Secondary electron emission: Part I. Secondary electron emission of metals," Physica **5**, 17–30 (1938).

[21] A. Kawano, "Effective work functions for ionic and electronic emissions from mono- and polycrystalline surfaces," Progr. Surf. Sci. **83**, 1–165 (2008).

[22] P. L. Lévesque, H. Marchetto, T. Schmidt, F. C. Maier, H.-J. Freund, and E. Umbach, "Correlation between substrate morphology and the initial stages of epitaxial organic growth: PTCDA/Ag(111)," J. Phys. Chem. C **120**, 19271–19279 (2016).

[23] N. Srivastava, Q. Gao, M. Widom, R. M. Feenstra, S. Nie, K. F. McCarty, and I. V. Vlassiouk, "Low-energy electron reflectivity of graphene on copper and other substrates," Phys. Rev. B **87**, 245414 (2013).

[24] J. Cazaux, "Reflectivity of very low energy electrons (< 10 eV) from solid surfaces: Physical and instrumental aspects," J. Appl. Phys. **111**, 064903 (2012).

[25] E. Bauer, *Surface microscopy with low energy electrons* (Springer, New York, 2014).

[26] H. Hibino, H. Kageshima, F. Maeda, M. Nagase, Y. Kobayashi, and H. Yamaguchi, "Microscopic thickness determination of thin graphite films formed on SiC from quantized oscillation in reflectivity of low-energy electrons," Phys. Rev. B **77**, 075413 (2008).

[27] R. M. Feenstra, N. Srivastava, Q. Gao, M. Widom, B. Diaconescu, T. Ohta, G. L. Kellogg, J. T. Robinson, and I. V. Vlassiouk, "Low-energy electron reflectivity from graphene," Phys. Rev. B **87**, 041406 (2013).

[28] K. Man and M. Altman, "Low energy electron microscopy and photoemission electron microscopy investigation of graphene," J. Phys.: Condens. Matter **24**, 314209 (2014).

[29] J. A. Assimos and D. Trivich, "The photoelectric threshold, work function, and surface barrier potential of single-crystal cuprous oxide," Physica Status Solidi (A) **26**, 477–488 (1974).

[30] L. G. Caron, V. Cobut, G. Vachon, and S. Robillard, "Electron transmission through a dirty surface in low-energy spectroscopy experiments," Phys. Rev. B **41**, 2693–2698 (1990).

[31] G. Bader, G. Perluzzo, L. G. Caron, and L. Sanche, "Structural-order effects in low-energy electron transmission spectra of condensed Ar, Kr, Xe, N_2, CO, and O_2," Phys. Rev. B **30**, 78–84 (1984).

[32] D. P. Pappas, K.-P. Kämper, B. P. Miller, H. Hopster, D. E. Fowler, C. R. Brundle, A. C. Luntz, and Z.-X. Shen, "Spin-dependent electron attenuation by transmission through thin ferromagnetic films," Phys. Rev. Lett. **66**, 504–507 (1991).

[33] R. Zdyb, T. O. Menteş, A. Locatelli, M. A. Niño, and E. Bauer, "Inelastic mean free path from reflectivity of slow electrons," Phys. Rev. B **87**, 075436 (2013).

[34] G. Rovida, F. Pratesi, M. Maglietta, and E. Ferroni, "Chemisorption of oxygen on the silver (111) surface," Surface Science **43**, 230–256 (1974).